Porosity of Additive Manufacturing Parts for Process Monitoring*

J. A. Slotwinski[a] and E. J. Garboczi[b]

National Institute of Standards and Technology, Engineering Laboratory
[a]Intelligent Systems Division and [b]Materials and Structural Systems Division
100 Bureau Drive, Gaithersburg, MD 20899

Abstract. Some metal additive manufacturing processes can produce parts with internal porosity, either intentionally (with careful selection of the process parameters) or unintentionally (if the process is not well-controlled.) Material porosity is undesirable for aerospace parts - since porosity could lead to premature failure - and desirable for some biomedical implants, since surface-breaking pores allow for better integration with biological tissue. Changes in a part's porosity during an additive manufacturing build may also be an indication of an undesired change in the process. We are developing an ultrasonic sensor for detecting changes in porosity in metal parts during fabrication on a metal powder bed fusion system, for use as a process monitor. This paper will describe our work to develop an ultrasonic-based sensor for monitoring part porosity during an additive build, including background theory, the development and detailed characterization of reference additive porosity samples, and a potential design for *in-situ* implementation.

Keywords: Additive Manufacturing, Porosity, Archimedes, X-Ray Computed Tomography, Ultrasonics, Non-Destructive Evaluation
PACS: 89.20 Bb

INTRODUCTION

The amount of porosity within parts produced via additive manufacturing (AM) is an area of interest in the AM community. Parts destined for high stress applications should be fully-dense, so as to minimize the possibility of part failure during service. On the other hand, a degree of porosity, especially surface-breaking porosity, is sometimes desirable and can be intentionally engineered into certain bio-medical implants, since the pores promote better osseointegration with biological tissue [1]. These requirements highlight the need for a real-time *in-situ* porosity monitoring capability, where the absolute level of porosity in a part can be measured and controlled while it is being built. In addition, even relative measurements of the changes in the porosity of a part during fabrication provides useful process information, since it may be an indication that the AM process is adversely changing and needs real-time adjustment.

In this paper, we present foundational research aimed at developing a real-time, *in-situ* ultrasonic sensor for monitoring changes in porosity in metal cobalt-chrome (CoCr) parts during additive manufacturing, for process monitoring. Previously published models that establish the relationship between the ultrasonic wavespeed in a material and the degree of porosity in that material are presented, and are used to calculate the measurement resolution needed to detect small changes in porosity. The construction and ultrasonic measurements of CoCr reference samples, made via an additive manufacturing powder bed fusion process, are described. Several different methods for measuring the samples' density (and hence their porosity) are then applied and compared, since accurate and precise measurements of wavespeed and porosity are necessary to be able to develop an accurate and precise

*Certain commercial equipment, instruments, or materials are identified in this paper to foster understanding. Such identification does not imply recommendation or endorsement by the National Institute of Standards and Technology, nor does it imply that the materials or equipment identified are necessarily the best available for the purpose.

relationship between the two. Finally, correlations between the part porosity and ultrasonic wavespeed measurements, along with a preliminary *in-situ* porosity sensor design for use in a metal powder bed fusion system, are presented.

ULTRASONICS BACKGROUND

Ultrasonic non-destructive evaluation (NDE) methods are useful for measuring the intrinsic properties of a material as well as detecting the presence of internal material defects such as cracks or pores. Conceptually similar to sonar, ultrasonic transducers use piezoelectric elements to convert electric signals to pressure waves. These same elements can then convert the reflected ultrasonic pressure waves back into an electrical signal. This allows a single ultrasonic transducer to serve as both transmitter and receiver (also known as "pulse-echo"). Signal frequencies are typically in the MHz range, and ultrasonic longitudinal wavespeeds in metals are on the order of 6 mm/μs (> 13,000 mi/h) [2]. With rapid measurement repetition frequencies (on the order of kHz), small sensor geometries, and low cost sensors that only require one-sided access to the parts under measurement, ultrasonic sensors are ideal for many *in-situ* measurement applications.

There is an abundance of material in the scientific literature that models ultrasonic wavespeed in a solid material as a function of the amount of porosity. This includes linear models that incorporate elastic theories for materials with low levels of uniform spherical porosity, as well as non-linear models that use wave scattering theories to take into account the shape and orientation of the pores [3,4,5,6,7,8,9]. We applied several of these theories, both linear and non-linear, to cobalt-chrome and found that an absolute change in porosity of 0.2% should be revealed by a change in velocity of -20 m/s. For a 10 mm thick sample, this results in a change in the measured time-of-flight of 0.01 μs, which is at the threshold of detectability for modest ultrasonic laboratory equipment.

REFERENCE SAMPLES

Since ultrasonic waves are sensitive to many different material properties (e.g., porosity, density, modulus, defects), it is critically important to have good reference samples that are independently characterized. For this work sixteen CoCr reference samples were made via a Direct Metal Laser Sintering (DMLS) additive manufacturing process. The samples were cylindrical disks, 40 mm in diameter and 10 mm thick. The porosity of these parts was controlled by varying the hatch speed and spacing during the DMLS build, and the target porosities ranged from 0% to 70%, although only two samples were intended to have porosities greater than 16%. These two highest porosity samples were later found to not be measureable by ultrasonic pulse-echo techniques as the high level of porosity scattered the ultrasonic waves to such as degree that no coherent reflected signals returned to the ultrasonic transducer. Subsequent to the ultrasonic testing several 5 mm diameter cylinders were cut out of each disk with an electric discharge machine. These smaller cyclinders were used for the X-Ray computed tomography and Archimedes tests reported later in this paper. In addition, the fully-dense bulk density of the CoCr material was determined by using helium pycnometry on CoCr powder that was very similar to that used to make these specimens. These measurements, which are detailed elsewhere [10], gave a CoCr density of 8.3046 g/cm^3 ± 0.0013 g/cm^3, where the measurement uncertainty has a k = 2 coverage factor, representing two standard deviations uncertainty, based on three independent measurements [11].

INDEPENDENT POROSITY MEASUREMENTS

Three different methods were used to measure the porosity of the 14 CoCr disks that were amenable to ultrasonic wavespeed measurements. A fourth method, digital analysis of surface and cross-section images, was used to confirm the presence of pores inside the samples. These results will be reported at a later date.

Method I: Archimedes

The Archimedes method is a classic approach for determining the density of a sample, using

$$\rho = \left(\frac{M_a}{M_a - M_w}\right)\rho_W \qquad (1)$$

where ρ_W is the density of water, M_a is the mass of the sample as measured in air, and M_w is the mass of the sample as measured in water. Once the density is measured, if the bulk density is also known, then the sample's porosity can be calculated. Since the density of water changes by only 2 parts per 1000 over the temperature range 15°C to 25°C, we took ρ_W to be 1 g/cm^3 [12]. A commercial Archimedes instrument was used on the small 5 mm diameter cylindrical samples that were cut out of the larger disks, and each cylindrical sample was measured multiple times. In addition to the porosity of each cylindrical sample, a composite disk porosity value was also determined from the individual cylindrical porosity values. This is a relatively simple method to measure porosity, but results could be affected by both microscopic air bubbles in the water as well as infiltration of the water into any surface-breaking pores.

Method II: X-Ray Computed Tomography (XRCT)

X-ray computed tomography (XRCT) is a technique that obtains X-ray images through a sample as it is rotated. The specimen is subjected to X-rays from many angles by rotating the specimen through approximately 1000 small angular increments between 0 and 360^o [13]. Reconstruction algorithms yield a sequence of 2-D gray level images (slices) perpendicular to the vertical axis of the cylindrical specimens that represent differences in the attenuation (which is dependent mostly on density) of different points within it. These slices can be computationally stacked to yield a 3-D view of the specimen. A commercial XRCT instrument with a 160 kV maximum voltage and a maximum power of 10 W was used to image one 5 mm diameter cylindrical sample from each of the fourteen disks. Each scan took roughly 5 hours, using a pixel resolution of about 2.5 μm.

Figure 1(a) shows a representative scan of one slice through one of the 5 mm cylinders. The actual dimension of the shown area is approximately 2.4 mm. Several localized areas of porosity, as well as cracks, can be seen. Figure 1(b) shows the porosity for each of 800 slices taken on one cylindrical sample, calculated by thresholding the image pixels into light and dark, corresponding to solid material and pores, and then dividing the number of dark pixels by the total number of pixels in each slice. Note that the three different curves show the porosity calculations taken in three different directions (z is perpendicular to Figure 1(a)). Again the localized variations in porosity are readily apparent, therefore an average porosity is computed.

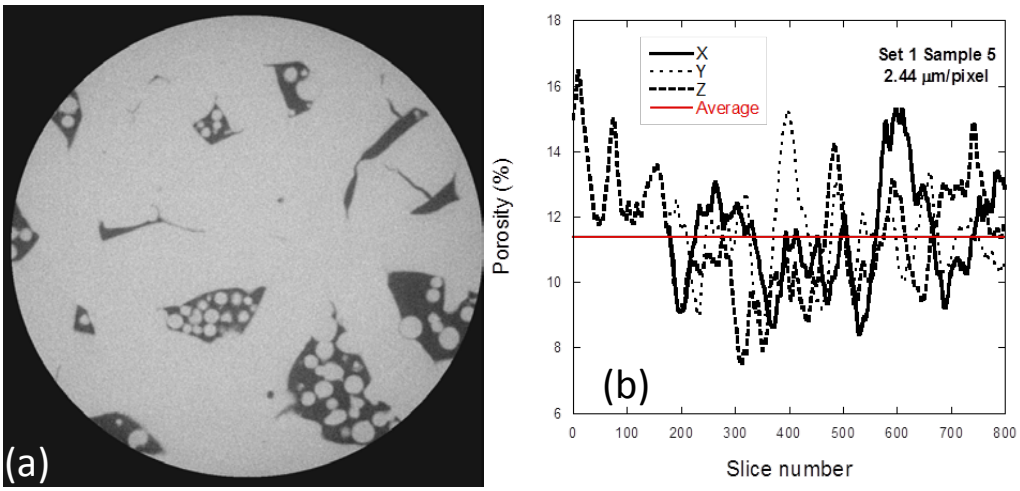

FIGURE 1. (a) XRCT slice image from 5 mm CoCr cylindrical sample. The diameter of the image is roughly 2.4 mm. (b) Porosity for each slice, calculated in three different directions, for one 5 mm CoCr cylindrical sample.

Method III: Mass and Volume

Straight-forward mass and volume measurements are the most simple ways to measure material density, and hence porosity, assuming that the fully-dense density is known. We measured the masses and volumes of both the entire 40 mm disks, before the cylindrical samples were removed, as well as that of the removed 5 mm cylinders. The individual cylinder porosities were also used to calculate a composite porosity for each of the disks.

COMPARISON OF RESULTS OF METHODS I - III

Figures 2 – 4 show comparisons of porosity measurements between the various methods reported in this paper. The error bars represent two standard deviations uncertainty. Figure 2 compares the results for the individual cylinders, as measured by the Archimedes and Mass/Volume methods. Overall there is good agreement, but there are some instances of discrepancy, perhaps due to the effects of water infiltration during the Archimedes measurements. Figure 3 compares the composite disk porosity results using Archimedes, the mass/volume of the small cylinders, and mass/volume of the whole disks. The overall agreement is quite good. The large error bars on the mass/volume measurements derived from the individual cylinder measurements are due to the local variations in porosity that were evident while measuring individual cylinders. Figure 4 compares mass/volume, XRCT, and Archimedes for 14 individual cylinders, one from each disk. The agreement between these methods for individual cylinders is quite good.

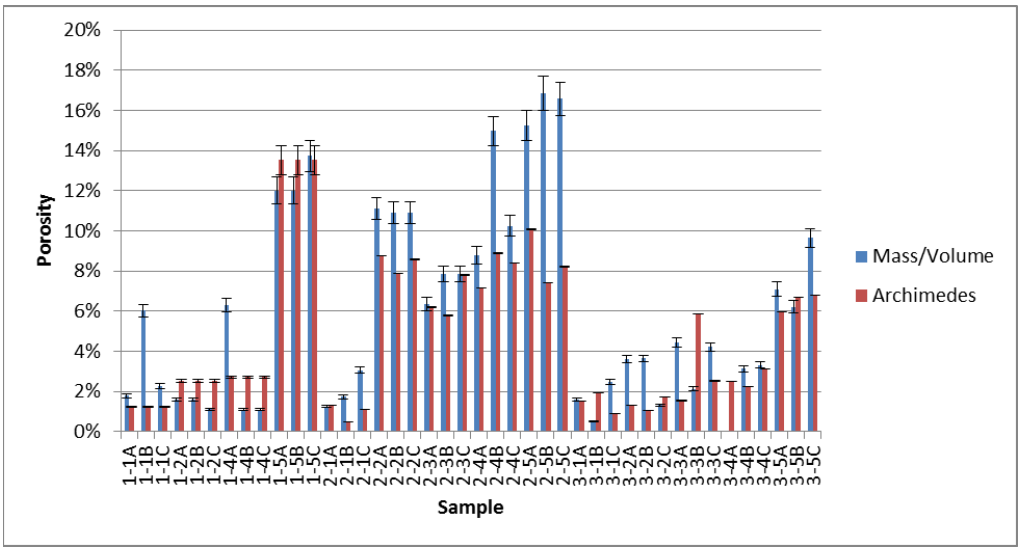

FIGURE 2. Comparison of mass/volume and Archimedes measurements of porosity for each of the 5 mm diameter cylindrical samples.

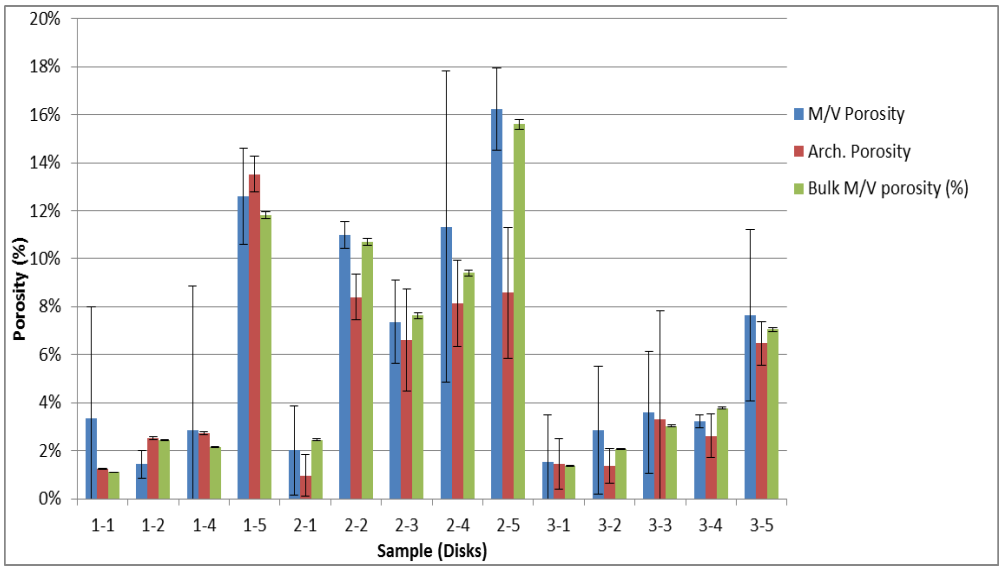

FIGURE 3. Comparison of mass/volume and Archimedes porosity measurements for each disk, taken from the disks' individual cylindrical porosity measurements, as well as the bulk disk porosity measurement from its own mass and volume.

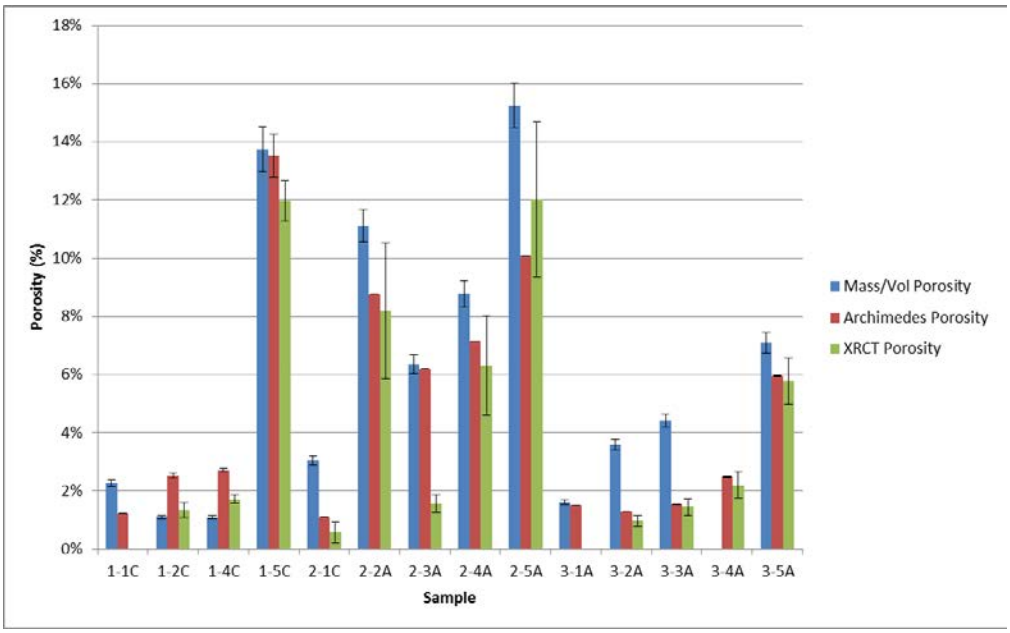

FIGURE 4. Comparison of porosity measurement for one representative 5 mm cylinder taken from each disk.

ULTRASONIC WAVESPEED MEASUREMENT TECHNIQUE

A 5 MHz contact transducer with a 12.7 mm diameter element size was used, along with a 30 MHz ultrasonic pulser/receiver. Although pulse-echo, through-transmission, and immersion techniques [14] were all tried, the results were all similar. Only the pulse-echo results are shown here. A 300 MHz bandwidth digital scope with a sample rate of 2.5 Giga samples per second was used to make three independent measurements for each sample. Each time record was an average of at least 512 signal acquisitions. The round trip time-of-flight was measured between successive back echoes using the echoes' first positive peaks and the digital scope's cursors. The resolution of the travel time measurement was 0.005 μs, better than that required to detect a 0.2% absolute change of porosity in a 10 mm thick CoCr sample.

Figure 5 shows the ultrasonic wavespeed as a function of measured porosity as determined using the bulk mass and volume (Method III). The data has been fit to a straight line of the form $v = v_o + \beta\varphi$ where v_o is the fully-dense velocity, φ is the material porosity, and β is the linear fit coefficient. Similar results were obtained when plotting the experimental wavespeed data against porosity determined by the other methods. These results are summarized in Table 1.

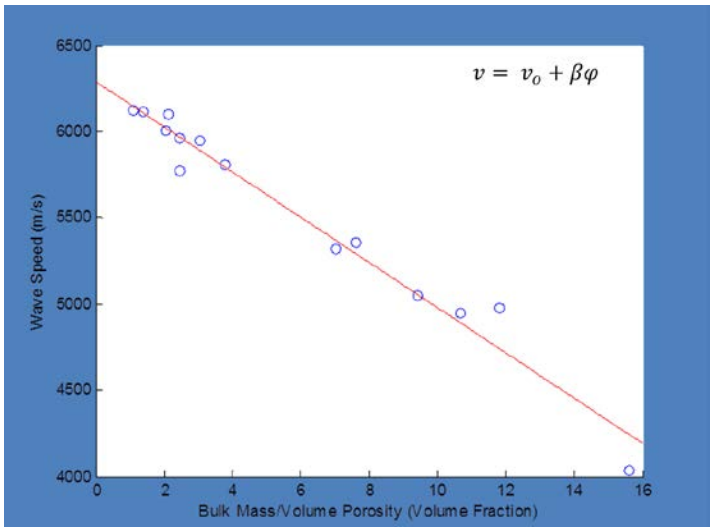

FIGURE 5. Ultrasonic wavespeed as a function of porosity where the porosity has been determined by the bulk mass and volume of each complete disk (Method III).

TABLE (1). Summary results showing dependence of ultrasonic wavespeed on porosity as determined by four different methods.

	Bulk Mass/Volume Porosity	Composite Mass/Volume Porosity	Archimedes Porosity	X-ray CT Porosity
Correlation R^2	0.9676	0.9295	0.6700	0.8265
v_o (m/s)	6292 (m/s)	6303 (m/s)	6181 (m/s)	6047 (m/s)
β (m/s/%)	-131.2 (m/s/%)	-123.3 (m/s/%)	-132.9 (m/s/%)	-132.0 (m/s/%)

CONCLUSIONS AND NEXT STEPS

The three methods for determining the porosity presented here generally agree, each method is different, and each has associated pros and cons. The ultrasonic velocity measurements reported here demonstrated sufficient sensitivity to detect small changes (~0.5%) in total porosity, and should be sensitive enough to detect process changes that cause such a change in the material porosity. One clear conclusion taken from both the XRCT images as well as the measurements of the individual cylinders cut from each disk is that the porosity in these samples is not uniformly distributed; the samples have clear local variations in porosity, both in the build direction and in the plane of each build.

We next plan to integrate an ultrasonic transducer into a DMLS machine. This will be done by adding two smaller build plates on top of the standard metal DMLS build plate, as shown in Figure 6. The middle plate will hold the ultrasonic transducer and wire. A sacrificial part, with a geometry amenable for ultrasonic wavespeed measurements, will be built on the top plate, along with whatever parts are being fabricated. The ultrasonic wavespeed in this part will be measured after each layer is melted, as a means of process monitoring.

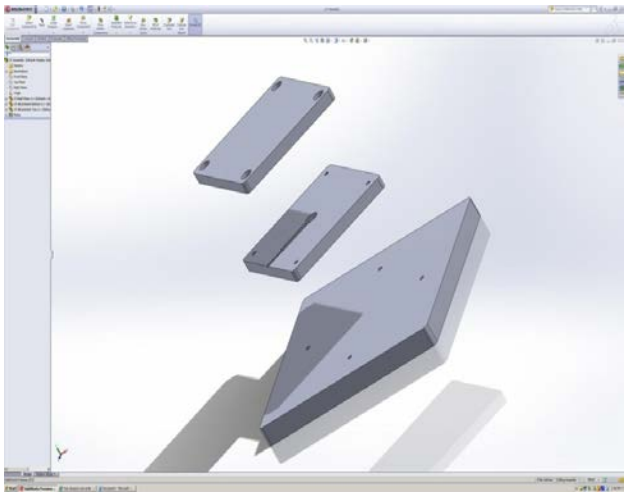

FIGURE 6. Design for incorporation of ultrasonic porosity sensor into DMLS machine.

REFERENCES

1. P. Heinl *et. al.*, Cellular Ti-6AL-4V Structures with Interconnected Macro Porosity for Bone Implants Fabricated by Selective Electron Beam Melting, Acta Biomaterialia **4**, 1536-1544 (2008). doi:10.1016/j.acbio.2008.03.013
2. L. Mordfin, ed., Handbook of Reference Data for Nondestructive Testing, ASTM International, 2002.
3. J. P. Panakkal, Use of Longitudinal Ultrasonic Velocity as a Predictor of Elastic Moduli and Density of Sintered Uranium Dioxide, IEEE Transactions on Ultrasonics, Ferroelectrics, and Frequency Control **38** (3), 161-165 (1991).
4. J. P. Panakkal, Nondestructive Characterization of Clay Ceramics using Ultrasonic, British Journal of NDT **34** (11), 529-532 (1992).
5. L.-S. Chang et al., Characterization of Alumina Ceramics by Ultrasonic Testing, Materials Characterization **45**, 221-226 (2000).
6. M. G. Hernandez et al., Application of a Micromechanical Model of Three Phases to Estimating the Porosity of Mortar by Ultrasound, Cement and Concrete Research **36**, 617-624 (2006).
7. D. N. Boccaccini and A. R. Boccaccini, Dependence of Ultrasonic Velocity on Porosity and Pore Shape in Sintered Materials, Journal of Nondestructive Evaluation **16** (4), 187-192 (1997).
8. W. Kreher et al., Ultrasonic Wave in Porous Ceramics with Non-Spherical Holes, Ultrasonics, 70-74 (March 1977).
9. J. A. Slotwinski and G. V. Blessing, Ultrasonic NDE of Sprayed Ceramic Coatings, Review of Progress in Quantitative Nondestructive Evaluation **15**, 1613-1620 (1996).
10. J. A. Slotwinski and P. E. Stutzman, *et. al.*, Physical and Chemical Characterization Techniques for Metallic Powders, Proceedings of the 40th Review of Progress in Quantitative Nondestructive Evaluation, 2013.
11. B. N. Taylor and C. E. Kuyatt, Guidelines for Evaluating and Expressing the Uncertainty of NIST Measurement Results, NIST Technical Note 1297, 1994.
12. Handbook of Chemistry and Physics, 58th Edition, 1977-1978.
13. A. C. Kak and M. Slaney, Principles of Computerized Tomographic Imaging, SIAM, New York, 2001
14. Nondestructive Testing: Ultrasonic, Classroom Training Handbook CT-6-4, 2nd Edition, General Dynamics, 1981.